Calibration and Performance of the ATLAS Tile Calorimeter During the LHC Run 2

Krystsina Petukhova (krystsina.petukhova@cern.ch), Charles University, Prague, Czech Republic
on behalf of the ATLAS collaboration

No. 272

The TileCal at the ATLAS experiment (LHC)

- Central section of hadronic calorimeter at the ATLAS experiment.
- Provides information for reconstruction of hadrons, jets, hadronic decays of tau-leptons and missing transverse energy.
- Assists in muon and electron identification.
- Composed by altering layers of active medium (plastic scintillator, tile) and absorber (steel).
- The charged particles passing through the tiles produce the light transmitted by wavelength shifting fibers to photomultiplier tubes (PMTs).

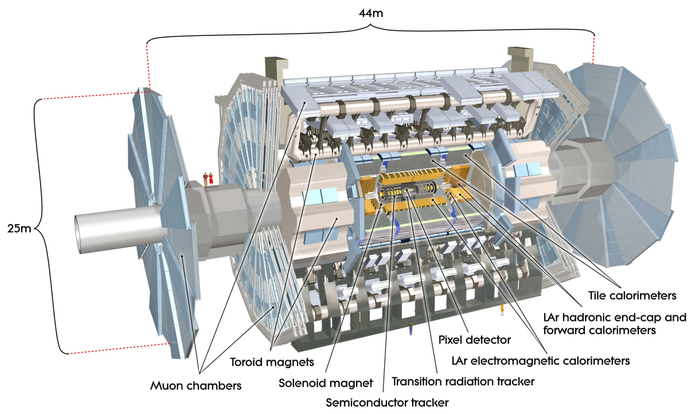

Figure 1: Cut-away view of the ATLAS experiment [1].

Signal reconstruction and calibration systems

- Segmented longitudinally and transversally into 5182 cells; a typical cell is readout by two PMTs (2 channels).
- The signal is passed to front-end electronics (FEE) for shaping, amplification (2 gains), digitization (10-bit ADC).
- The Optimal Filter (OF) algorithm reconstructs the amplitude and time of the signal in a given event.
- Deposited energy is evaluated based on measured ADC-counts and calibration coefficients.

$$A = \sum_{i=1}^{7} a_i S_i \quad \tau = \sum_{i=1}^{7} b_i S_i \qquad E[\mathrm{GeV}] = A[\mathrm{ADC}] \cdot C^{\mathrm{CIS}}_{\mathrm{ADC}\to\mathrm{pC}} \cdot C_{\mathrm{laser}} \cdot C_{\mathrm{Cs}} \cdot C_{\mathrm{pC}\to\mathrm{GeV}}$$

  - The electromagnetic (EM) scale $C_{\mathrm{pC}\to\mathrm{GeV}}$ is measured during the test beam campaigns.
  - C_{Cs} determines the response of the scintillating tiles and slow FEE readout with a Cesium (Cs) radioactive source.
  - C_{laser} measures the response of PMTs, optic and fast FEE path with a Laser light system.
  - $C^{\mathrm{CIS}}_{\mathrm{ADC}\to\mathrm{pC}}$ is provided by Charge Injection system for FEE.
- Alternative Wiener Filter (WF) algorithm has been recently designed for more robust energy reconstruction under high pile-up condition in specific scintillator cells (Figure 3).
- The TileCal calibration systems monitor the detector status and provide a means for equalizing the calorimeter response at each stage of the signal propagation.

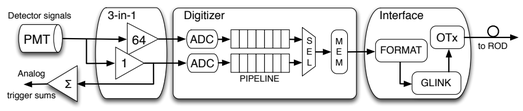

Figure 2: The TileCal FEE layout [2].

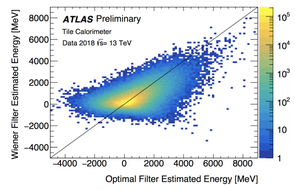

Figure 3: Energy reconstructed with the OF and WF [3].

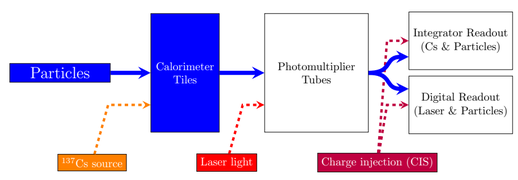

Figure 4: The TileCal calibration flow diagram [4].

Cesium calibration

- Cs radioactive sources go through a system of steel tubes traversing all the tiles; C_{Cs} quantifies the produced light yield w.r.t. to the EM scale determined in beam tests.
- The response is corrected for natural Cs decay over time, magnetic field effect, and accounts for varying size of the TileCal cells.

Laser calibration

- Laser constant C_{laser} depends on the PMT response and optical and electronic path state.
- Mean gain variation is below 2.5% for a standard cell (Figure 5).
- Laser light shots during empty bunches are used for the monitoring synchronization between LHC clock and digitization time.

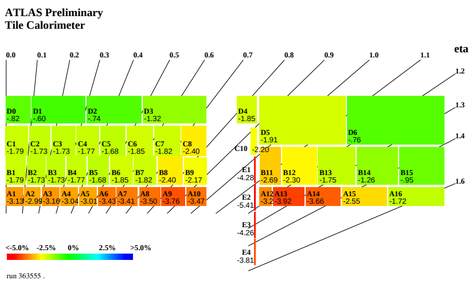

Figure 5: The mean gain variation between the end and start of 2018 *pp* collisions [4].

Charge Injection calibration

- CIS constant $C^{\mathrm{CIS}}_{\mathrm{ADC}\to\mathrm{pC}}$ measured as ADC-count response to an analog charge injected by FEE DAC.
- Scaling factor about 81.28 ADC/pC for high gain (1.27 ADC/pC for low gain) with typical variation of ∼1.6% among all channels (Figure 7) and systematic uncertainty.
- The RMS variation over the entire Run 2 of detector-wide $C^{\mathrm{CIS}}_{\mathrm{ADC}\to\mathrm{pC}}$ is 0.03-0.04% (Figure 6).

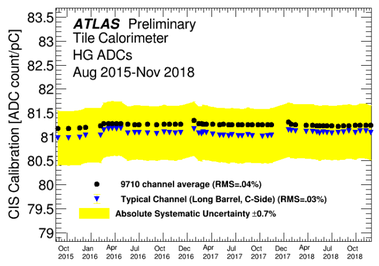

Figure 6: Evolution of CIS calibration constants in the entire Run 2 [4].

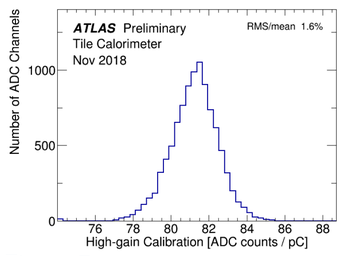

Figure 7: Distribution of in a single 2018 run [4].

Minimum Bias calibration

- The Minimum Bias system gives information about instantaneous luminosity and monitors full optical route.
- Integrator calibration reveals the functionality of slow readout path and FEE.

Combined energy calibration

- Gain variation is confirmed in laser, Cs, Minimum Bias calibrations.
  - While the Laser calibration only sees the PMT response degradation due to current, the Min Bias sees in addition the scintillator light yield loss due to radiation. This explains the difference between the two responses in Figure 8.
- The response drifts down during physics collisions due to scintilator aging due to radiation, and PMT gain loss due to current. During the LHC stops and shutdowns the response drifts up as the PMT gain recovers.

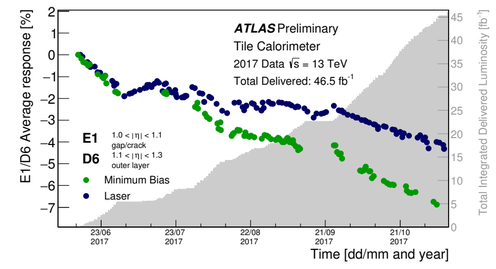

Figure 8: Evolution of response in Minimum Bias and Laser calibration [4].

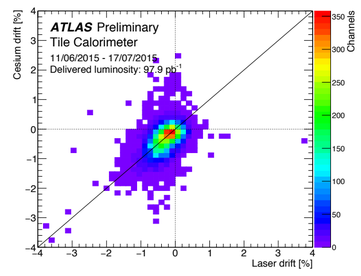

Figure 9: Gain variation observed by Laser and Cesium systems [4].

Single particle response

- The response of high momentum isolated cosmic muons verifies the measured energy at the EM scale, isolated hadrons are used as a probe of the hadronic response.
- The detector response uniformity (Figure 10) and linearity (Figure 11) are observed.

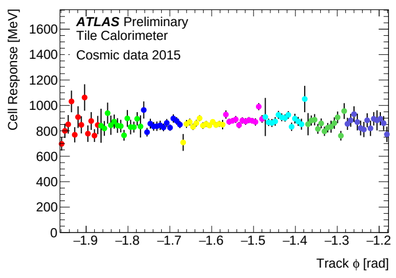

Figure 10: Cosmic muon energy deposition profile as a function of track ϕ impact point [5].

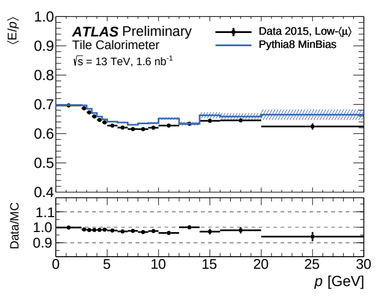

Figure 11: Response to isolated hadrons as a function of momentum [6].

Noise and timing performance

- The electronic noise is measured to be at the level of 20-40 MeV, in dedicated pedestal runs without signal exposure.
- The pile-up noise is measured with zero-bias triggered events and compared to minimum bias Monte Carlo (MC) simulations (Figure12).
- The time resolution studied with multijet events is within 1 ns for the cell with energy input above 30 GeV (Figure 13).

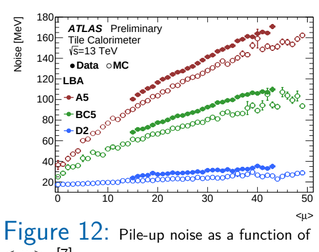

Figure 12: Pile-up noise as a function of $< \mu >$ [7].

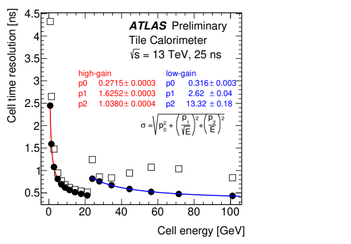

Figure 13: TileCal time resolution vs. E_{cell} [8].

pp collisions measurements

- Jet energy scale is estimated with the proton-proton collision data.
- Jet energy resolution is within designed $\frac{\sigma}{E} = \frac{50\%}{\sqrt{E}} \oplus 3\%$ (Figure 15).
- Energy profile is well modeled by MC methods (Figure 14).

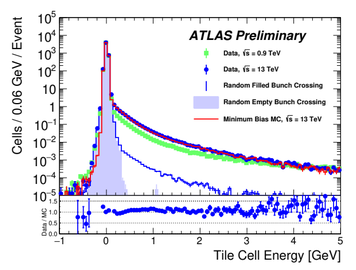

Figure 14: TileCal cell energy deposition [9].

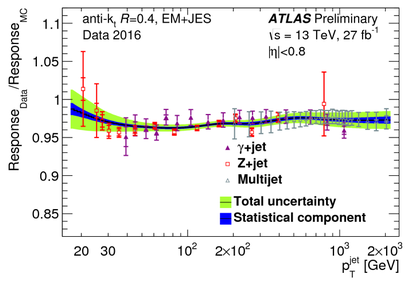

Figure 15: Ratio of jet response in data & MC [10].

Detector status

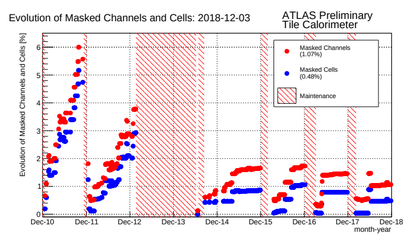

Figure 16: Evolution of cell masking [11].

- The faulty channels are not used in further energy reconstruction.
  - 0.46% of cells and 1.05% of channels were masked at the end of the Run 2 (Figure 16).
- Data Quality (DQ) efficiency is above 99% for the entire Run 2.

References

1. https://twiki.cern.ch/twiki/bin/view/AtlasPublic/AtlasTechnicalPaperListOfFigures/
2. https://twiki.cern.ch/twiki/bin/view/AtlasPublic/ApprovedPlotsTileElectronics/
3. https://twiki.cern.ch/twiki/bin/view/AtlasPublic/ApprovedPlotsTileSignalReconstruction
4. https://twiki.cern.ch/twiki/bin/view/AtlasPublic/ApprovedPlotsTileCalibration/
5. https://twiki.cern.ch/twiki/bin/view/AtlasPublic/ApprovedPlotsTileEnergyCalibration
6. https://twiki.cern.ch/twiki/bin/view/AtlasPublic/ApprovedPlotsTileSingleParticleResponse/
7. https://twiki.cern.ch/twiki/bin/view/AtlasPublic/ApprovedPlotsTileNoise/
8. https://twiki.cern.ch/twiki/bin/view/AtlasPublic/TileCaloPublicResultsTiming
9. https://twiki.cern.ch/twiki/bin/view/AtlasPublic/ApprovedPlotsTileEnergyDeposition
10. https://atlas.web.cern.ch/Atlas/GROUPS/PHYSICS/PLOTS/JETM-2017-003/
11. https://twiki.cern.ch/twiki/bin/view/AtlasPublic/ApprovedPlotsTileDetectorStatus